

EFFECT OF MORTAR TYPE AND WORKMANSHIP ON THE BEHAVIOUR OF MASONRY UNDER UNIAXIAL COMPRESSION

¹R. HENDRICKX, ²L. SCHUEREMANS, ¹E. VERSTRYNGE,
²K. VAN BALEN, ²D. VAN GEMERT

¹ Ph.D. researcher

² Prof. Dr. Ir.

Katholieke Universiteit Leuven
Department of Civil Engineering
Heverlee, Belgium

SUMMARY

Small changes in water to binder ratio of mortar introduce uncertainty in the performance of masonry. The effect of this variation and of the workmanship of the mason is examined in an extensive experimental programme involving 6 masons of 3 different nationalities, 7 types of binders, 42 sets of mortar prisms and 42 masonry columns. The results are used to assess the validity of the formula proposed in Eurocode 6 for calculation of masonry strength from the strength of the components for this specific case, and to compare the differences in the behaviour of masonry made with mortars with different binder types.

INTRODUCTION

Contrary to lab practice, mortars produced on site may have a slightly varying water content from one batch to another. These variations bring about differences in the hardened state which affect the properties of the masonry such as the strength, stiffness, ductility, crack formation and propagation, and the final collapse mode. This effect is different depending on the type of mortar used.

The effect of workmanship on the hardened state of masonry is even more difficult to quantify. The interaction between the workability of the mortar and the “modus operandi” of the workman may seem evident at first sight, but is rather complex because a lot of variables are involved. Workmanship includes the pre-conditioning of the bricks, the mixing procedure, the way in which the mortar bed is spread, how the brick is put in place, until what extent horizontal and vertical joints are filled up. It interrelates with the workability of the mortar because a specific way of working requires a stiffer or more liquid consistency. This can be adjusted by the mason – for a given dry composition and admixture dosage – by varying the water to binder ratio (W:B). The way a mortar is squeezed out of a joint, whether and how much the bricks are tapped, may affect the stability of the mortar mix and have consequences for the bonding between the brick

and the joint. It is generally assumed that there are important national and regional differences in masonry workmanship and hence also in the choice for mortar consistence.

The mechanical properties of the mortar and the units are often used to predict the strength of masonry. A wide variety of mostly empirical models is discussed in literature (Binda et al. 1988, Dymiotis and Gutleiderer 2002, Schueremans 2001). These model formulas can be extended to assess the variations in masonry behaviour, resulting from the uncertainty in mortar strength. The formula proposed in Eurocode 6 (equation 3.1) is applied to the experimental results, in this case for a high strength brick and medium strength mortars (Eurocode 6 2002). A quantification of the spread of results is particularly relevant, because it affects the characteristic values to a large extent.

The primary motivation for the experimental programme with a number of masons is an interest in workability of the fresh mortars. For this purpose, also low strength lime-based mortars are included. The results of this workability research are discussed elsewhere.

MATERIALS AND METHODS

The 7 types of binders and their binder to aggregate ratio (B:A) are listed in Table 1. Their chemical composition is given in Table 2. Binder 7 is used in 2 subsets of mortars with a different dosage of air entraining agent: 0.4% of the binder weight in 7a and 0.1% of the binder weight in 7b. Plasticizer is added at 0.5% of the binder weight. The aggregate is a siliceous quarry sand 0/0.5 (0/1) (EN 13139:2002), a so-called “Lommel” type of sand from a quarry in Zutendaal, Belgium, and is one of the typically used aggregates for masonry in the region (Figure 1). The unit is a small size fired clay facing brick, type Mono 3009 by Vandemoortel, Belgium, with nominal dimensions 19x9x5 cm³ (LxBxH).

Table 1. Description of binders

N°	Name	Description	Binder mass on 1m ³ of dry aggregate (kg/m ³)	B:A (kg/kg)
1	CL 90	calcic lime CL90 (EN 459-1:2001)	180	0.127
2	CL90 + PZ + HB	calcic lime (75%) with hydraulic binder (15%) and pozzolana (10%)	280	0.197
3	CL 90 + AEA	calcic lime CL90 (EN 459-1:2001) with air entraining agent	180	0.127
4	CL 90 + CEM I 42.5 R	calcic lime CL90 (EN 459-1:2001) (66.7%) and ordinary Portland cement CEM I 42.5 R (33.3%)	300	0.212
5	NHL 5	natural hydraulic lime NHL 5 (EN 459-1:2001)	300	0.212
6	CEM I 42.5 R	ordinary Portland cement CEM I 42.5 R	350	0.247
7	CEM I 42.5 R + SP + AEA	ordinary Portland cement CEM I 42.5 R with commercial additives: plasticizer Rheomix 359 and air entraining agent Micro-air 100 (BASF)	350	0.247

The masonry is produced by six masons with at least 5 years of experience in using lime mortars. The panel is composed of three nationalities: mason 1, 5 and 6 are Belgian, Dutch speaking; mason 2 is French; mason 3 is Dutch and mason 4 is Belgian, French speaking. The chosen binder to aggregate ratios (B:A) (Table 1) are derived from a practice-based reference and are recalculated with the measured bulk densities to mass ratios.

Table 2. Chemical composition of binders by wet analysis (binder 7: identical to binder 6)

	1	2	3	4	5	6
	CL 90	CL90 + PZ + HB + AEA	CL 90 + AEA	CL 90 + CEM I 42.5 R	NHL 5	CEM I 42.5 R
Free Ca(OH) ₂ (%)	70.35	27.26	*	23.05	1.75	2.25
SO ₃ (%)	0.38	1.67	0.25	2.22	2.14	3.39
CaO (%)	73.94	66.01	72.81	67.32	44.8	62.48
MgO (%)	0.83	0.73	1.09	1.17	2.39	1.34
SiO ₂ (%)	0.34	8.16	1.11	11.51	18.58	14.64
Fe ₂ O ₃ (%)	0.12	1.32	0.23	2.32	1.71	3.42
Al ₂ O ₃ (%)	0.08	1.77	0.07	2.05	3.56	3.07

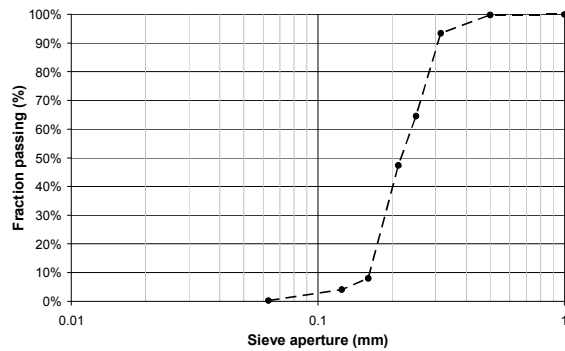


Figure 1. Grain size distribution of aggregate

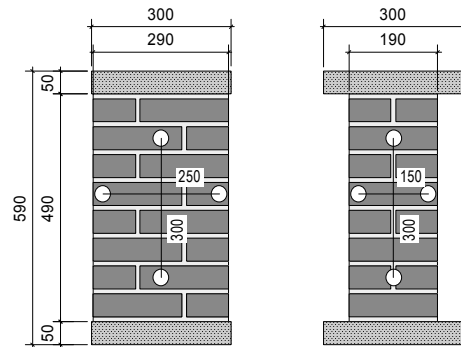


Figure 2. Geometry of columns

The water to binder ratios (W:B) are not fixed, but they are chosen by each mason for each individual composition in order to achieve an optimum workability of the mortar. Mixing is done in a floor-model Hobart mixer type M80 (max. content ± 80 l) following a fixed procedure. Approximately 75% of the estimated needed water quantity is poured in the bowl, then half of the aggregate, the binder, and the other half of the aggregate are added. Mixing is done at low speed, while water is added, until water content and homogeneity are optimal.

The consistence of each composition is measured immediately by plunger penetration (EN 459-2:2001) and mortar prisms are produced (EN 196-1:1995). Prisms with binder 1 to 3 are cured in the covered moulds for 10 days and for 80 more days in lab conditions 20°C and relative humidity of 60%. Prisms with binder 4 to 6 are cured for 7 days (demoulded after 24 h) at high relative humidity (92%) and then cured for 83 days in lab conditions. Masonry columns are made of 24 bricks in alternating bond between two concrete tiles (Figure 1). The columns with hydraulic mortars are wrapped in plastic sheet until 24 h after production, when the top tile is placed. Curing is done in lab conditions for 90 days.

All mechanical experiments are carried out at an age of 90 ± 2 days. The mortar prisms are tested for flexural tensile strength f_{mf} , compressive strength f_{mc} (EN 196-1:1995) and dynamic Young's

modulus E_{dyn} by ultrasonic wave velocity (NBN B15-229:1976). The masonry units are tested for compressive strength f_{bc} (EN 772-1:1999), and additionally $4 \times 4 \times 16 \text{ cm}^3$ prisms cut from the brick are used to measure tensile strength f_{bt} and flexural strength f_{bf} . Masonry columns are subjected to a displacement controlled compressive test at $v=0.2 \text{ mm/min}$ on a Dartec hydraulic press (maximum capacity 5000 kN). Driving force and deformation were continuously recorded by the force cell of the press and 8 linear variable differential transducers (LVDTs), 1 vertical and 1 horizontal on each side of the columns (Figure 2).

RESULTS AND DISCUSSION

Table 3 gives the W:B selected by the masons for each binder type. For each binder type, the W:B values for the different masons are relatively close to each other, with a coefficient of variation (COV) between 3% and 10% only. The agreement between the masons is best for binders 1 and 3 (air lime), and worst for binder 6 (cement). We can evaluate the “water need” of one particular mason by normalizing his W:B scores with the average and spread of all masons (Equation 1).

$$Z_{\text{mason } x, \text{ binder } y, N} = (W:B_{\text{mason } x, \text{ binder } y} - W:B_{\text{average, binder } y}) / \sigma_{W:B, \text{ all masons, binder } y} \quad (1)$$

Assuming a normal probability distribution for the water content chosen by a large population of masons for one mortar, and adopting the experimental average and standard deviation as best estimators, the resulting variable Z is normally distributed (Montgomery and Runger 1994). The average and standard deviation of the Z variable are listed in table 4.

Table 3. water to binder ratio selected by masons and measured plunger penetration (PP) for mortars with different types of binders

	binder	W:B mean	W:B COV	PP mean (cm)	PP COV
1	CL 90	2.02	3%	2.2	20%
2	CL90 + PZ + HB	0.90	6%	1.9	35%
3	CL 90 + AEA	1.48	4%	2.7	23%
4	CL 90 + CEM I 42.5 R	1.00	6%	2.7	33%
5	NHL 5	1.13	7%	2.6	22%
6	CEM I 42.5 R	0.93	10%	2.3	17%
7a	CEM I 42.5 R + SP + AEA	0.70	-	2.7	-
7b	CEM I 42.5 R + SP + AEA	0.79	9%	2.7	15%

These values can be interpreted as follows: mason 1 usually chose a W:B towards the lower end of the range, but was not very consistent in doing so. Mason 2, 3 and 5 used higher W:B than average and mason 4 and 6 lower than average. This water need for the masons can be correlated to the working method, which is summarised in Table 4. The jointing is done immediately after bricklaying and with the same mortar.

Table 4. Working methods of masons related to normalised water need

	filling of horizontal joints	filling of vertical joints	way of placing brick	average Z value W:B	Z standard deviation
mason 1 (B, D)	nearly complete	incomplete	tapping with blade of trowel	-0.690	1.370
mason 2 (F)	complete	complete (from above)	tapping with rubber hammer	0.358	0.826
mason 3 (N)	complete	complete (if possible when laying the brick)	only by hand, extruding the mortar by pressing	0.791	0.539
mason 4 (B, F)	nearly complete	nearly complete	mostly by hand, light tapping with handle of trowel	-0.315	0.598
mason 5 (B, D)	incomplete	smeared from the side on brick in position	tapping with blade of trowel	0.194	0.439
mason 6 (B, D)	incomplete	nearly complete; on brick in position and new brick	tapping with handle of trowel	-0.383	0.641

It may be clear that the method of mason 3 requires a more fluid mortar to enable him to extrude the excess mortar by hand. Otherwise the pressure on the wrist would become too high. On the other hand, mason 1, 5 and 6 apply an incomplete filling of the joints, which means a more local application of the mortar bed: a smaller force has to be exerted on the brick to lower it in the bed, hence the lower average Z-value (Table 4). The average Z value for mason 4 is low compared to his working method; this corresponds however with the observation that he preferred, from his professional point of view, to apply a higher force than average rather than use more water.

The results of the plunger penetration test (Table 3) on the fresh mortars show a very large variance (COV from 15% to 43 %) with average values fluctuating around 2,5 cm. This variance is typical for this type of test and can be related to the large influence of small differences in the way of execution, that are difficult to exclude. As expected, mason 3 had consistently the highest value. Indeed, for the differences between the masons, the same considerations as for W:B are valid.

The results of mechanical tests on the mortar prisms are given in Table 5. The prisms of mortar of binders 1, 3 and 5 have a very low compressive strength f_{mc} (between 0.8 and 1.0 MPa) and flexural strength f_{mf} . There is a high correlation for all mortars between f_{mc} and f_{mf} (Figure 3a), with an exception for binders 1, 3 and 5. Their score well below the overall regression line can be explained by the anisotropic behaviour of the prisms: the outer layer, which is carbonated to a certain extent, has a higher stiffness and strength than the inner material. The result is a non-linear stress distribution over the section in the flexural test and a “hollow tube effect” which explains the slightly better performance in the flexural test. These findings are more pronounced for the air lime (binder 1 and 3) than for the natural hydraulic lime (binder 5), which developed a more homogeneous strength (Figure 3b).

The differences in W:B between the masons have consequences for the strength of the mortar prisms. The compressive strength for binder 4, 6 and 7 shows a clear decrease for increasing W:B. This influence is not significant for the air lime (binder 1 and 3), nor – more surprisingly – for the natural hydraulic lime (binder 5). The same dependency was found for the dynamic Young's modulus of the prisms. As for binder 7: subset 7a has obviously a lower strength

because of the higher porosity. We propose the dynamic Young's modulus (derived from propagation of ultrasound waves) as an indicator for the static Young's modulus (stress over strain ratio), although the relation between both is not evident and usually E_{stat} is lower than E_{dyn} (Stark and Wicht 2000). It can be noted in the mortars of binder 3 versus 1 and 7a and 7b versus 6, that the influence of porosity on E_{dyn} is less pronounced than for f_{mc} and f_{mf} (Table 5).

Table 5. Mechanical properties of mortar prisms

	binder 1	binder 2	binder 3	binder 4	binder 5	binder 6	binder 7a	binder 7b
	CL 90	CL90 + PZ + HB + AEA	CL 90 + AEA	CL 90 + CEM I 42.5 R	NHL 5	CEM I 42.5 R	CEM I 42.5 R +SP+AEA	CEM I 42.5 R +SP+AEA
f_{mc} mean (MPa)	1.00	4.68	0.81	7.35	0.82	17.02	11.73	14.45
f_{mc} COV	9%	29%	11%	9%	7%	17%	-	9%
f_{mf} mean (MPa)	0.83	2.26	0.65	3.46	0.52	7.36	6.34	6.61
f_{mf} COV	16%	21%	16%	6%	16%	16%	-	9%
$E_{\text{m, dyn}}$ mean (MPa)	3688	7991	3159	9361	2342	15608	13289	14071
$E_{\text{m, dyn}}$ COV	5%	19%	5%	7%	5%	10%	-	5%
n	6	6	6	6	6	6	2	4

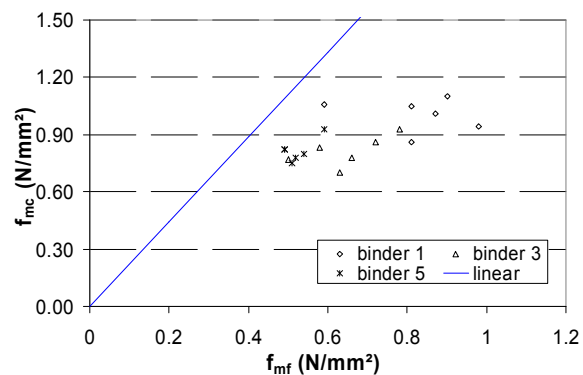
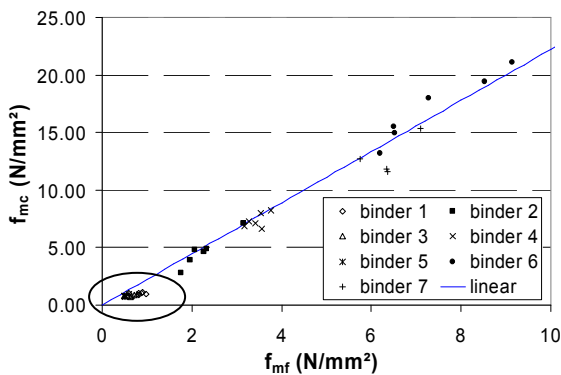
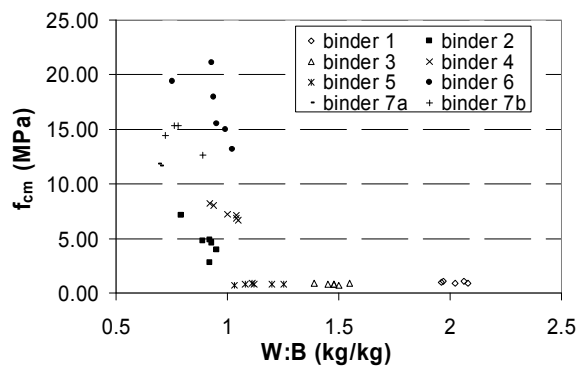
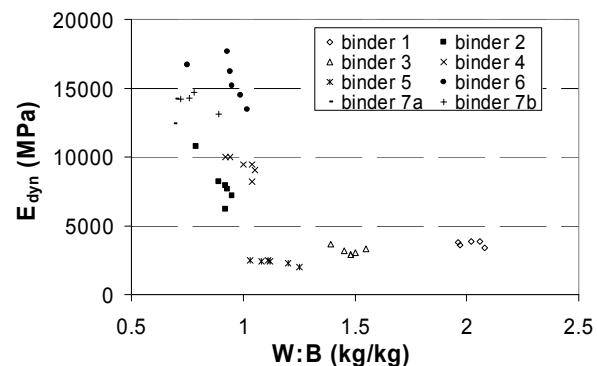


Figure 3a and 3b. Flexural strength versus compressive strength of mortar prisms: overview of all mortars (left, a) and detail of lower end (right, b)

Figure 4. f_{mc} as a function of W:BFigure 5. E_{dyn} as a function of W:B

The experimentally determined compressive strength of the columns f_{wc} ranges from 5 to 35 MPa (Table 6). The first cracks appear around 60% to 75% of the maximum force for the weaker mortars, and around 85% to 100% of the maximum force for the strongest mortars. The strain at which this crack occurs tends to be low if the corresponding stress is high, and vice versa. Cracking starts in the middle of the narrow sides of the column, as a vertical splitting crack in the brick, and develops gradually in vertical direction. Cracks in the wide sides start at higher stress levels and develop more locally. Two clearly different failure modes are distinguished: sudden collapse by brittle failure of the inner structure (columns with binders 6, 7a, 7b); or gradual (ductile) failure with small drops in stress at very high deformation (columns with binders 1, 3 and 5). In the first mode, collapse is not always preceded by standard crack development. The columns made with mortars of binder 2 and 4 show intermediate failure modes.

Table 6. Experimental results of masonry compressive tests

binder	statistic	f_{wc} (MPa)	σ_{crack} (MPa)	$\epsilon_{\sigma max}$ (mm/m)	E_{sec33} (MPa)	ν_{33}	$E_{tan 40}$ (MPa)	ν_{40}
1 (n=6)	mean	8.69	6.02	9.25	1472	0.14	1102	0.15
CL 90	COV	8%	12%	14%	13%	16%	18%	11%
2 (n=6)	mean	17.53	13.73	5.54	8833	0.20	5183	0.23
CL90 + PZ + HB + AEA	COV	6%	12%	16%	13%	20%	20%	27%
3 (n=6)	mean	5.59	4.40	14.80	1222	0.15	592	0.16
CL 90 + AEA	COV	13%	23%	34%	24%	26%	37%	25%
4 (n=6)	mean	23.72	20.43	4.11	13297	0.19	9052	0.24
CL 90 + CEM I 42.5 R	COV	11%	19%	34%	6%	36%	13%	29%
5 (n=6)	mean	14.58	9.48	7.89	3874	0.17	2014	0.20
NHL 5	COV	14%	24%	16%	24%	18%	14%	15%
6 (n=6)	mean	34.07	31.22	3.23	14544	0.19	12319	0.26
CEM I 42.5 R	COV	18%	21%	11%	12%	18%	12%	14%
7a (n=2)	mean	28.88	21.87	3.07	12516	0.15	11373	0.25
CEM I 42.5 R +SP+AEA	COV	-	-	-	-	-	-	-
7b (n=4)	mean	37.35	35.89	3.23	15697	0.19	12805	0.25
CEM I 42.5 R +SP+AEA	COV	8%	8%	14%	9%	8%	6%	12%

In general the ratio of masonry strength between the different binders, is far inferior to the corresponding ratio in mortar strength. The resulting stress-strain diagrams typically show an early start of horizontal deformation at the narrow sides, and later for the wide sides (Figure 6). The onset of cracking is not visible in the vertical deformation curve. All curves are consistently non-linear due to damage accumulation: the Young's modulus decreases continuously upon development of cracks in the structure. They also show a vertical segment at the lower end and a subsequent inclination, due to gradual force redistribution at the start of the test, which explains the large difference between the secant Young's modulus for 33% of the strength and the tangent Young's modulus at 40% of the strength. The first is calculated by dividing stress by strain at $0.33f_{wc}$, the latter by subtracting the values at $0.35f_{wc}$ from those at $0.45f_{wc}$. The corresponding values were used to calculate the Poisson ratios ν_{33} and ν_{40} . By visual comparison of the stress-strain diagrams a more linear behaviour can be distinguished for the columns with weaker mortars versus a more inclined behaviour for the stronger mortars (Figure 7).

The low strength mortars result in masonry columns with low Young's modulus and high deformation before the first crack appears. The Poisson ratio for these columns is lower than average, while we would expect initially a more or less constant value, when conservation of volume and a similar deformation mechanism are assumed. The lower value can be attributed to a different collapse mechanism. At the end of the compression tests the joints of these columns were pulverised, also at several centimetres distance from the surface. These observations suggest that there is a volume decrease in the joints, due to collapse of the binder matrix and rearranging of the packing of the aggregate grains.

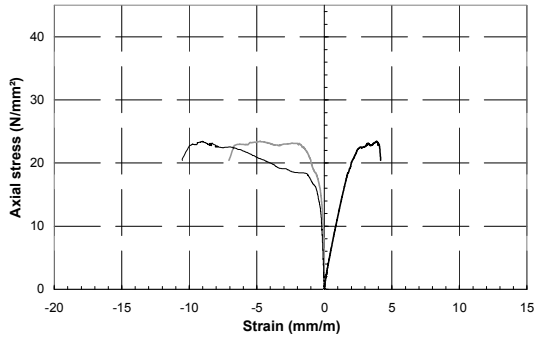


Figure 6. Typical stress-strain diagram of masonry column (mason2, binder 6)

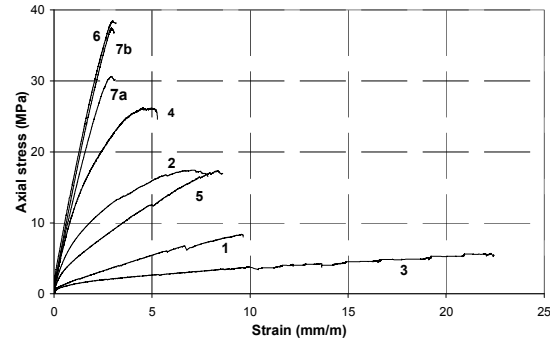


Figure 7. Stress-strain diagrams of a typical series of columns with different binders (mason 3)

The effect of workmanship on f_{wc} may be due to the different choice of W:B (Table 1) of the mortars and due to the different working methods (Table 4). There is however no clearly visible relation between f_{wc} and f_{mc} in the experimental results (Figure 8). This means that the negative correlation between W:B and f_{mc} for hydraulic mortars, is not found in f_{wc} .

The effect of the working method of the mason is assessed for the mortars which are not influenced by W:B, i.e. the mortars with binder 1, 3 and 5 (Figure 9). We expect a higher average score for mason 3, who pays most attention to a complete filling of joints and avoiding tapping of the bricks. This is confirmed by the experiments, although mason 4, who also takes care to work in a similar way, does not achieve a higher value than average. It is surprising on the other hand that masons 1, 5 and 6, who work with an incomplete filling of horizontal and vertical joints when laying the bricks, do not have the lowest scores. The lower values of mason 2 and 4 can not be related to simple observation.

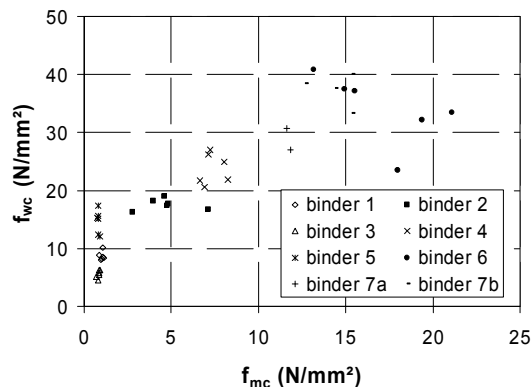


Figure 8. f_{wc} as a function of f_{mc}

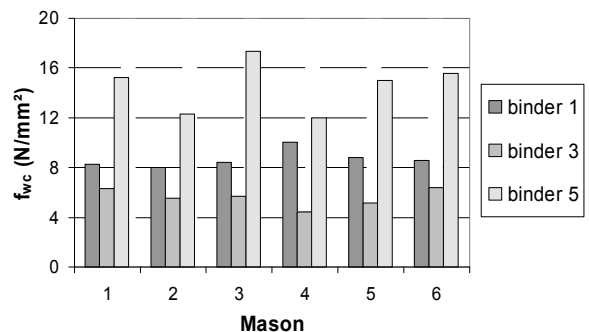


Figure 9. Strength of masonry

The effect of the differences in type of binder is most evident for the low strength mortars (mortars with binder 1, 3 and 5). The surprising absence of a clear relationship between f_{mc} and f_{wc} can be explained from the different nature of the hardening mechanisms of the air hardening lime and the natural hydraulic lime. Carbonation of the lime mortar after 90 days is only superficial, which gives larger benefit for f_{mc} , but only a limited increase for f_{wc} . This means that the validity of models based on f_{mc} to determine f_{wc} is questionable for this type of mortars at this age of the masonry. This is confirmed by tests with phenolphthalein as pH indicator on sections of the columns. The colour transition after 95 days is located at greater depth for binder 5 (26mm) than for binder 1, 3 and 4 (6 to 13mm) or binder 2 (17mm).

The consequences of variations due to the effect of workmanship and binder type for model predictions can be quantified by comparing the experimental variance to the variance calculated from the model. We evaluate the formula proposed in Eurocode 6 for the case of the columns with binders 2, 4, 6 and 7 (equation 2). The Eurocode formula has been shown to be one of the most reliable and practically usable formulas available in literature (Schueremans 2001). The mortars with binder 1, 3 and 5 are below the strength range of these formulas and are left out of the further analysis. The quantity f_{wc} is a characteristic value, which corresponds to the 5th percentile in a fitted probability distribution, while f_{bc} and f_{mc} are mean values (where f_{bc} is corrected with a shape factor δ) (Eurocode 6 2002).

$$f_{wc} = K \cdot f_{bc}^{0.65} f_{mc}^{0.25} \quad (2)$$

K is a shape coefficient and is equal to 0.5 in this case. The expected value μ , the standard deviation σ and the 5th percentile of strength values are calculated based on a lognormal distribution. The expected variance σ^2 of the logarithmic transformation of f_{wc} can be calculated as (Table 8) (Schueremans and Van Gemert 2006):

$$\sigma_{\ln f_{wc}}^2 = 0.65^2 \sigma_{\ln f_{bc}}^2 + 0.25^2 \sigma_{\ln f_{mc}}^2 \quad (3)$$

$$\sigma_{f_{wc}}^2 = \mu_{f_{wc}}^2 ((\exp \sigma_{\ln f_{wc}}^2) - 1) \quad (4)$$

Table 8. Masonry strength: experimental values and values calculated from EC6 model

Mortar: $f_{mc,exp}$ (MPa)					
	binder 2	binder 4	binder 6	binder 7a	binder 7b
	CL90 + PZ + HB + AEA	CL 90 + CEM I 42.5 R	CEM I 42.5 R	CEM I 42.5 R +SP+AEA	CEM I 42.5 R +SP+AEA
μ	4.72	7.36	17.06	11.73	14.46
σ	3.16	2.28	8.02	-	4.64
Bricks: $f_{bc,exp}$ (MPa) $\mu = 83.56$ $\sigma = 5.03$ ($\delta = 0.82$)					
Masonry experimental: $f_{wc,exp}$ (MPa)					
μ	17.53	23.74	34.22	28.94	37.38
σ	1.02	2.68	6.76	-	3.01
$f_{wc,exp,0.05}$	16.38	19.73	24.79	-	32.75
Masonry numerical model: $f_{wc,mod} = K \cdot f_{bc}^{0.65} \cdot f_{mc}^{0.25}$ (MPa) (K=0.50)					
μ	12.96	14.60	17.98	-	17.29
σ	1.12	0.65	1.06	-	0.78
n	6	6	6	2	4

The calculated values of $f_{wc,mod}$ are well below the experimental expected value $f_{wc,exp}$, and range from 54 to 81% of the characteristic value derived from it $f_{wc,exp,0.05}$. This means that for this particular case with high strength bricks, the formula is conservative, despite the relatively large contribution of brick strength to the result. The standard deviations obtained experimentally are higher than the values obtained from calculations of the model formula (equation 3), and have a considerable variance. In this case, which can simulate a working site with several masons or small fluctuations in mortar batches, it is the mortar strength which has the highest coefficient of variation of both components, with an average COV of 14%, versus 6% for the brick. The experiments on the masonry yield an average COV of 11%, while the model predicts only 5%.

SYNTHESIS AND CONCLUSIONS

The free choice of W:B for masons introduced a variation in the composition in the mortar for masonry. This variation in W:B is larger for cement-based binders, than for lime-based binders. A relationship has been demonstrated between the W:B chosen by a mason and his personal working method. This was confirmed by plunger penetration tests, despite the large spread on the results. Mortar prisms with these varying W:B behave differently according to the nature of the binder used. The lime mortars show an influence of anisotropy due to the process of carbonation, while the hydraulic mortars show a decrease of strength with increasing W:B. The amount of air voids plays an equally important role.

These differences in mortar strength could not be correlated to the strength of the masonry. Masonry columns displayed two distinguished failure modes, depending on the strength and stiffness of the mortar used. For the weakest mortars, a low lateral expansion was observed, which suggests an internal failure and volume decrease by denser packing of the mortar. This assumption was confirmed by observations during the experiments.

The use of the model given in Eurocode 6 for prediction of masonry strength from the strength of the components, was applied to the results, and proven to be conservative for expected value in this case. The model underestimates the experimental value in all cases. The opposite is true for the variance calculated from the model: here a lower value was predicted than the experimental value. This suggests that caution is needed when using the formula for similar cases.

ACKNOWLEDGEMENTS

Lhoist R&D (Nivelles, B.) is gratefully acknowledged for their financial support of the research. Our gratitude goes also to the technical staff of the Laboratorium Reyntjens (Heverlee, B.) for the meticulous way in which the experiments were carried out, to Vandemoortel (Oudenaarde, B.) for supplying the bricks, and to the contractors who took part in the experimental programme: De Bont (Vucht, NL), Building (Geel, B), Verstraete&Vanhecke (Wilrijk, B), Corda (Battice, B), Monument Vandekerckhove (Ingelmunster, B), Huger (Le Mans, Fr).

REFERENCES

Binda, L., Fontana, A., and Frigerio, G., “Mechanical behaviour of brick masonries derived from unit and mortar characteristics”, *8th international brick/block masonry conference*, Dublin, 1988, pp. 136-147.

Dymiotis, C.; Gutleiderer, B. M., “Allowing for uncertainties in the modelling of masonry compressive strength”, *Construction and building materials*, Vol. 16, 2002, pp. 443-452.

Eurocode 6 - Design of masonry structures - Part 1-1: General rules for buildings - Rules for reinforced and unreinforced masonry with Belgian application document included, CEN, Brussels, 2002.

Montgomery, D.C., Runger, G.C. *Applied statistics and probability for engineers*, Wiley, New York, 1994.

Schueremans, L., *Probabilistic evaluation of structural unreinforced masonry*, Ph.D., Katholieke Universiteit Leuven, Leuven, 2001.

Schueremans, L. and Van Gemert, D., “Probability density functions for masonry material parameters - a way to go?”, in: Lourenço, P.B., Roca, P., Modena, C., and Agrawal, S. *Structural analysis of historical constructions* (Vol. 2), New Delhi, 2006, pp. 921-928.

Stark, J. and Wicht, B., *Zement und Kalk*, Birkhäuser, Basel, 2000.